

Combined Design and Robust Control of a Vehicle Passive/Active Suspension

Sulaiman F. Alyaqout, Panos Y. Papalambros, and A. Galip Ulsoy

Abstract—System performance can significantly benefit from optimally integrating the passive and active elements of vehicle suspension systems. The present article introduces an approach that combines passive and active elements to improve the robustness of a vehicle suspension system with respect to a worst-case scenario. This integrated passive and active suspension approach leads to a coupled optimization problem that is often difficult to solve. To reduce the computational effort, a sequential strategy that optimizes the passive elements first, and then the active elements, is used depending on the strength of the coupling. The effect of level of uncertainty, tire stiffness, and unsprung mass parameters on this coupling is then studied. Varying such parameters leads to establishing a relationship between coupling and robustness of the control system. This link between coupling and robustness can be utilized to aid the designer in assessing the parameters' influence on coupling and robustness. Results show that the coupling between design and robust control tends to increase as the level of uncertainty increases. In addition, demanding more robustness for vehicle suspensions with harsh ride characteristics increases coupling much more rapidly compared to suspensions with soft ride characteristics.

Index Terms—coupling, design, robust control, combined design and control

I. INTRODUCTION

The design of vehicle suspension systems is influenced by several conflicting performance requirements. Such requirements include isolating passengers from road disturbances to improve ride comfort and maintaining good road holding to improve vehicle handling. For optimization problems, these requirements are often represented by a weighted performance function [1], [2]. Active suspensions can better resolve the tradeoffs among these conflicting performance requirements because they have the ability to not only store and dissipate, but also to introduce energy into the system. As a result, active suspensions outperform passive suspensions [2], [3], [4]. On the other hand, active suspensions require suitable actuator devices and high levels of energy-consumption leading to an increase in system costs. To reduce such costs, and to ensure “limp-home” performance in case of active suspension failure, it is desirable to combine passive and active elements in a suspension.

S. F. Alyaqout is with the Department of Mechanical Engineering, The University of Michigan, Ann Arbor, MI 48109-2125 (e-mail: alyaqout@umich.edu).

P. Y. Papalambros is with the Department of Mechanical Engineering, The University of Michigan, Ann Arbor, MI 48109-2125 (e-mail: pyp@umich.edu).

A. G. Ulsoy is with the Department of Mechanical Engineering, The University of Michigan, Ann Arbor, MI 48109-2125 (e-mail: ulsoy@umich.edu).

Another critical requirement for active suspension design is to improve the robustness of the suspension system. Many active suspension control approaches have been proposed, utilizing various modern control techniques, such as linear-quadratic (LQ) [5], linear-quadratic-gaussian (LQG) [5], [6], adaptive control [7], and nonlinear control [8]. However, in practice the total mass of the vehicle is uncertain due to changes in passenger and cargo loads, and the damping of the vehicle is uncertain due to approximating the nonlinear model with a linear one, etc. As a result, robust control synthesis for active suspension systems has been investigated by several researchers [9], [10]. Recently, several authors employed \mathcal{H}_∞ -based control to improve the robustness properties and disturbance attenuation of active suspensions [11], [12]. The problem with \mathcal{H}_∞ -based controllers is that they are typically too conservative [13].

Several authors have examined strength-based coupling between design and control optimization problems [14], [15], [16]. Alyaqout [17], [18], Reyer [19], and Fathy [20] proposed the use of optimality conditions to characterize coupling. In Alyaqout [18], we defined coupling relative to the solution method, by comparing the optimality conditions of a sequential design and robust control solution strategy with the optimality conditions of the undecomposed system optimization problem. Hence, this coupling was shown to have a direct effect on determining the system optimum. In addition, we related coupling between design and robust control to the robustness of the control system.

Much of the research in modern control of active suspensions has been concerned with robust control. Robust control assumes that the passive design variables are parameters that should not be modified during the controller design process. Therefore, the effect of the passive design variables in improving the robustness of the control system is ignored. In addition, most previous characterizations of coupling fail to incorporate uncertainty. By incorporating this uncertainty, Alyaqout [18] introduced an original relationship between coupling and robustness, which is applied here to the vehicle suspension system case study.

In the present article the design and robust control of a vehicle passive/active suspension system is examined via the relationship between coupling and robustness resulting from varying different suspension parameters. Section II presents the two degree-of-freedom quarter-car vehicle suspension model used for the study. Section III poses the system problem under consideration. In Section IV, we study the relationship between coupling and robustness. In Section V, we examine the frequency response of the suspension. The

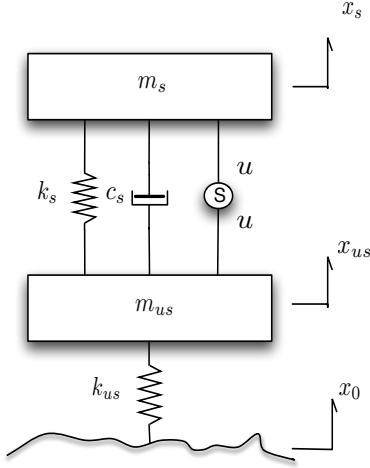


Fig. 1. Quarter-car model for an active suspension system

article concludes with a discussion of results and future work.

II. VEHICLE SUSPENSION MODEL

The suspension dynamics are based on a linear time-invariant (LTI) two degree-of-freedom quarter-car model, Figure 1. In this model, m_s and m_{us} are the sprung and unsprung masses, k_s and c_s are the passive suspension stiffness and damping coefficient, and k_{us} is the tire stiffness. Moreover, x_s , x_{us} and x_0 are the vertical displacements of the sprung mass, the unsprung mass and the road, respectively. The dynamics of the quarter-car model can be described by

$$\dot{\mathbf{x}}(t) = \mathbf{A}\mathbf{x}(t) + \mathbf{B}u(t) + \mathbf{D}w(t) \quad (1)$$

where \mathbf{A} , \mathbf{B} , \mathbf{D} are the system matrix, control matrix and disturbance matrix, respectively, which are given by

$$\mathbf{A} = \begin{bmatrix} 0 & 1 & 0 & 0 & -1 \\ -k_{us} & -c_s & k_s & c_s & 0 \\ m_{us} & m_{us} & m_{us} & m_{us} & 0 \\ 0 & -1 & 0 & 1 & 0 \\ 0 & c_s & -k_s & -c_s & 0 \\ 0 & m_s & m_s & m_s & 0 \\ 0 & 0 & 0 & 0 & -\omega_f \end{bmatrix}, \mathbf{B} = \begin{bmatrix} 0 \\ -1 \\ m_{us} \\ 0 \\ 1 \\ m_s \\ 0 \end{bmatrix}, \mathbf{D} = \begin{bmatrix} 0 \\ 0 \\ 0 \\ 0 \\ 0 \\ \omega_f \end{bmatrix} \quad (2)$$

and the state vector $\mathbf{x}(t)$ is

$$\mathbf{x}(t) = [x_{us} - x_0 \quad \dot{x}_{us} \quad x_s - x_{us} \quad \dot{x}_s \quad \dot{x}_0]^T \quad (3)$$

where $x_s - x_{us}$ is the suspension stroke, $x_{us} - x_0$ is the tire deflection and $u(t)$ is the scalar active force generated by an actuator. The ground motion $w(t) = \dot{x}_0(t)$ is a hypothetical zero-mean, white and Gaussian disturbance of variance $2\pi A_0 V$, where A_0 is a ground motion amplitude scaling factor and V is the vehicle forward velocity [5]. In addition, this ground motion $w(t)$ is acted upon by a first-order low-pass filter with cutoff frequency $\omega_f = 20.91$ to produce a colored ground disturbance velocity input [3]. Finally, we assume that all system states are available for feedback, therefore no observer is required.

III. THE DRC VEHICLE SUSPENSION PROBLEM

We now present a combined robust passive/active suspension problem written in the form of the design and robust control (DRC) formulation introduced by Alyaqout [18]. The design determines the passive suspension stiffness k_s and damping coefficient c_s , while the control determines the full state feedback controller gains. The objective is to improve performance robustness of a weighted sum of sprung mass acceleration, wheel hop, rattle space, and control effort while maintaining robust stability assuming uncertainty in the sprung mass m_s . Given the system dynamics in Eq. (1), consider the following active suspension DRC optimization problem

$$\min_{k_s, c_s, \mathbf{x}(t), u(t), \mathbf{K}} \max_{\Delta m_s} F = E \left(\int_{t_i}^{t_f} (r_0 \ddot{x}_s^2 + r_1 (x_{us} - x_0)^2 + r_2 (x_s - x_{us})^2 + r_3 u^2) dt \right)$$

subject to

$$\dot{\mathbf{x}}(t) = \begin{bmatrix} 0 & 1 & 0 & 0 & -1 \\ -k_{us} & -c_s & k_s & c_s & 0 \\ m_{us} & m_{us} & m_{us} & m_{us} & 0 \\ 0 & -1 & 0 & 1 & 0 \\ 0 & c_s & -k_s & -c_s & 0 \\ 0 & 0 & 0 & 0 & -\omega_f \end{bmatrix} \mathbf{x}(t) + \begin{bmatrix} 0 & 0 \\ -1 & 0 \\ m_{us} & 0 \\ 0 & 0 \\ 1 & 0 \\ 0 & \omega_f \end{bmatrix} \begin{bmatrix} u(t) \\ w(t) \end{bmatrix}$$

$$k_s \leq 160000, c_s \leq 16000 \quad (4)$$

$$1 - \alpha \leq \Delta m_s \leq 1 + \alpha, u(t) = -\mathbf{K}\mathbf{x}(t)$$

$$(k_s, c_s, \mathbf{x}(t), u(t), \mathbf{K}, \Delta m_s) \in \{$$

$$(k_s, c_s, \mathbf{x}(t), u(t), \mathbf{K}, \Delta m_s) : \text{eig}(\mathbf{A} - \mathbf{B}\mathbf{K}) \leq 0,$$

$$\text{for every } \Delta m_s \in \{\Delta m_s : 1 - \alpha \leq \Delta m_s \leq 1 + \alpha\}$$

where

$$\hat{m}_s = (m_s)(\Delta m_s), \quad E(w(t)w(\tau)) = 2\pi A_0 V \delta(t - \tau)$$

Here Δm_s is the real set-based uncertainty in the sprung mass $m_s \in \mathbb{R}$ with resulting variable $\hat{m}_s \in \mathbb{R}$ defined to represent percentage type uncertainty, F is the performance index, $E(\cdot)$ is the expected value operator, $\text{eig}(\cdot)$ is the eigen value of a matrix, δ is the Dirac delta function, and α is the level of uncertainty. The quantities r_0, r_1, r_2 and r_3 are parameters that weigh the sum of root mean square values of sprung mass acceleration \dot{x}_{4rms} , tire deflection (wheel hop) x_{1rms} , suspension stroke (rattle space) x_{3rms} and active control force [5], respectively. In addition, full state feedback is assumed and $\mathbf{K} \in \mathbb{R}^{1 \times 5}$ is the corresponding controller gain.

There are several challenges associated with solving the DRC optimization problem. The solution of this minimax optimization problem requires heavy computational effort even for modestly-sized problems, since the number of design variables under uncertainty increases the complexity of the optimization problem. In addition, the DRC can be a non-convex optimization problem even if the individual design and robust control optimization problems are convex.

Some of the problems associated with solving the DRC optimization problem can be avoided by utilizing a sequential

TABLE I

ACTIVE DRC AND SDRC SUSPENSIONS WITH VARIOUS RIDE CHARACTERISTICS FOR THE NOMINAL ZERO UNCERTAINTY CASE (S = SOFT RIDE, T = TYPICAL RIDE, AND H = HARSH RIDE)

	DRC/S	DRC/T	DRC/H	SDRC/S	SDRC/T	SDRC/H
Performance Index	31.15	321.97	1991.9	32.43	335.8	2039.8
$x_{1rms}/\sqrt{2\pi A_0 V}$	0.1962	0.076	0.0655	0.1676	0.06	0.066
$x_{3rms}/\sqrt{2\pi A_0 V}$	0.5921	0.319	0.208	0.582	0.3098	0.2125
$x_{4rms}/\sqrt{2\pi A_0 V}$	3.16	10.57	22.66	3.311	11.502	22.438
k_s (kN/m)	1.66	18.5	31.7	1.2	1.2	2.44
c_s (kN.s/m)	0.312	3.05	16.0	1.89	7.95	16.0
Controller Gain, $\mathbf{K}(10^3)$	13.88	63.2	4.92	13.93	55.4	11.72
	0.06	1.33	0.41	1.55	4.747	0.405
	13.7	64.7	57.7	14.17	81.85	81.6
	7.46	14.2	5.85	5.88	9.85	7.73
	-0.49	-2.12	-0.299	-0.425	-1.369	-0.572

strategy under uncertainty that often yields a suboptimal solution (i.e., improved solution but not optimal). Now we introduce such a sequential design and robust control (SDRC) strategy [18] to solve the DRC active suspension problem in Eq. (4). The SDRC strategy optimizes the design problem first. Then the design solution is used in the optimization of the robust control problem, thus saving time and cost. The design problem can be described as follows

$$\min_{k_s, c_s} E\left(\int_{t_i}^{t_f} (r_0 \ddot{x}_s^2 + r_1 (x_{us} - x_0)^2 + r_2 (x_s - x_{us})^2) dt\right)$$

subject to

$$k_s \leq 160000, \quad c_s \leq 16000 \quad (5)$$

where

$$\dot{\mathbf{x}}(t) = \mathbf{A}\mathbf{x}(t) + \mathbf{D}w(t), \quad E(w(t)w(\tau)) = 2\pi A_0 V \delta(t - \tau)$$

The design problem in Eq. (5) has no dependence on the control variables and parameters. This makes the problem easier to solve and removes the need for iteration between the design and robust control optimization problems.

After solving the design problem in Eq. (5), the resulting optimal solution is used to solve the following robust control problem

$$J(\mathbf{x}_d) = \min_{\mathbf{x}(t), u(t), \mathbf{K}} \max_{\Delta m_s} E\left(\int_{t_i}^{t_f} (r_0 \ddot{x}_s^2 + r_1 (x_{us} - x_0)^2 + r_2 (x_s - x_{us})^2 + r_3 u^2) dt\right)$$

subject to

$$\dot{\mathbf{x}}(t) = \begin{bmatrix} 0 & 1 & 0 & 0 & -1 \\ -k_{us} & -c_s & k_s & c_s & 0 \\ m_{us} & m_{us} & m_{us} & m_{us} & 0 \\ 0 & -1 & 0 & 1 & 0 \\ 0 & c_s & -k_s & -c_s & 0 \\ 0 & \hat{m}_s & \hat{m}_s & \hat{m}_s & 0 \\ 0 & 0 & 0 & 0 & -\omega_f \end{bmatrix} \mathbf{x}(t) + \begin{bmatrix} 0 & 0 \\ -1 & 0 \\ m_{us} & 0 \\ 0 & 0 \\ 1 & 0 \\ \hat{m}_s & 0 \\ 0 & \omega_f \end{bmatrix} \begin{bmatrix} u(t) \\ w(t) \end{bmatrix} \quad (6)$$

$$1 - \alpha \leq \Delta m_s \leq 1 + \alpha, \quad u(t) = -\mathbf{K}\mathbf{x}(t)$$

$$(k_s, c_s, \mathbf{x}(t), u(t), \mathbf{K}, \Delta m_s) \in \{$$

$$(k_s, c_s, \mathbf{x}(t), u(t), \mathbf{K}, \Delta m_s) : \text{eig}(\mathbf{A} - \mathbf{B}\mathbf{K}) \leq 0,$$

$$\text{for every } \Delta m_s \in \{\Delta m_s : 1 - \alpha \leq \Delta m_s \leq 1 + \alpha\}$$

where

$$\hat{m}_s = (m_s)(\Delta m_s), \quad E(w(t)w(\tau)) = 2\pi A_0 V \delta(t - \tau)$$

The robust control problem in Eq. (6) is affected by the design variables k_s, c_s and uncertainty associated with design parameter $m_s = 2000 \text{ kg}$. However, note that the values of k_s and c_s are fixed in Eq. (6). Since the robust suspension problem in Eq. (4) is written in terms of the DRC notation, then the DRC coupling Γ_R for the active suspension problem can be calculated as follows [18].

$$\Gamma_R = \left\| \frac{\partial J}{\partial \mathbf{x}_d} \right\|_2 \quad (7)$$

where $\mathbf{x}_d = (k_s, c_s)^T$ is the vector of design variables, $\|\cdot\|$ is the vector norm, J is the performance index as defined in Eq. (6). Thus, Γ_R reflects the sensitivity of the objective function at the optimum to the values of the design variables k_s, c_s .

A comparison of active DRC suspensions with various ride characteristics for the nominal zero uncertainty case ($\alpha = 0$) is presented in Table I. The selection of the weighting parameters r_0, r_1, r_2 and r_3 in the performance index F allows one to achieve these different ride characteristics [1]. Following Ulsoy [5], three ride characteristics are compared: the soft ride case (S) is found with $r_0 = 1, r_1 = 1, r_2 = 6, r_3 = 4 \times 10^{-9}$; the typical ride case (T) with $r_0 = 1, r_1 = 1, r_2 = 2 \times 10^3, r_3 = 4 \times 10^{-8}$; and the harsh ride case (H) with $r_0 = 1, r_1 = 3 \times 10^4, r_2 = 3 \times 10^4, r_3 = 4 \times 10^{-6}$. The soft ride (DRC/S) is characterized by low sprung mass rms acceleration, large rms suspension stroke, and large rms tire deflection. The harsh ride (DRC/T) case provides low suspension stroke and tire deflection, but at the expense of high sprung mass rms acceleration. The typical ride (DRC/T) case has medium sprung mass acceleration, suspension stroke, and tire deflection compared to the soft and harsh ride cases. The corresponding SDRC suspensions are also shown in Table I.

IV. RELATIONSHIP BETWEEN COUPLING AND ROBUSTNESS FOR THE VEHICLE SUSPENSION SYSTEM

We examine now the effect of parameters on coupling and robustness of the control system. The DRC coupling in Eq. (7) depends on several parameters that were first

defined in the DRC optimization problem in Eq. (4). Varying these parameters establishes a relationship between the DRC coupling and the robustness of the control system. This link between coupling and robustness can be utilized to aid the designer in assessing the parameters' influence on coupling and robustness. In this section, the effect of the level of uncertainty parameter α on coupling and robustness is investigated first. Then, the effect of varying the tire stiffness parameter k_{us} and the unsprung mass parameter m_{us} on the relationship between coupling and robustness is studied.

A. Relationship Between Coupling and Robustness Resulting from Varying the Level of Uncertainty in the Sprung Mass

Because the uncertainty in m_s affects both design and control decisions, a relationship between coupling and control robustness exists. The relationship between coupling and robustness can be found by varying the level of uncertainty α . The level of uncertainty $\alpha \in [0, 1]$ is used to vary the size of the uncertainty set for the DRC problem.

The DRC coupling defined in Eq. (7) can be interpreted as a measure of the degree to which the SDRC solution can achieve the DRC solution. The importance of the DRC coupling stems from the direct effect it has on the location of the DRC robust system solution.

Alternatively, another measure of coupling can be defined by comparing the optimal worst-case performance of the design and robust control (DRC) problem with the optimal worst-case performance of the sequential design and robust control (SDRC) problem. Let F_{SDRC}^* represent the optimal worst-case objective obtained using the SDRC strategy, and F_{DRC}^* represent the optimal worst-case objective obtained using the DRC strategy. Then the coupling strength measure can be defined as the absolute difference between the optimal worst-case performances of the SDRC and DRC strategies $|F_{DRC}^* - F_{SDRC}^*|$.

Figure 2 illustrates the relationship between coupling computed using Eq. (7) and level of uncertainty α for different ride characteristics. Figure 3 illustrates the relationship between coupling and level of uncertainty α by comparing the difference between the optimal worst-case performances of the DRC and SDRC strategies for different ride characteristics. The two figures illustrate the usefulness of the coupling in measuring the difference between the SDRC and DRC solutions. There are several interesting observations to be made from the results in Figures 2 and 3. For all ride characteristics, the DRC coupling increases as the level of uncertainty α is increased. Hence, one can conclude that increasing the uncertainty level α tends to increase the coupling between design and robust control, so solving the DRC in Eq. (4) is advantageous compared to solving the SDRC in Eq. (5) and Eq. (6) for high robustness requirements.

The ride characteristics of the vehicle suspension system also has an effect on coupling. The soft ride case (DRC/S) in Figure 2 has a slope of 2.35. The typical ride case (DRC/T) has an increased slope of 19. While, the harsh ride case (DRC/H) has the largest slope value of 105. As

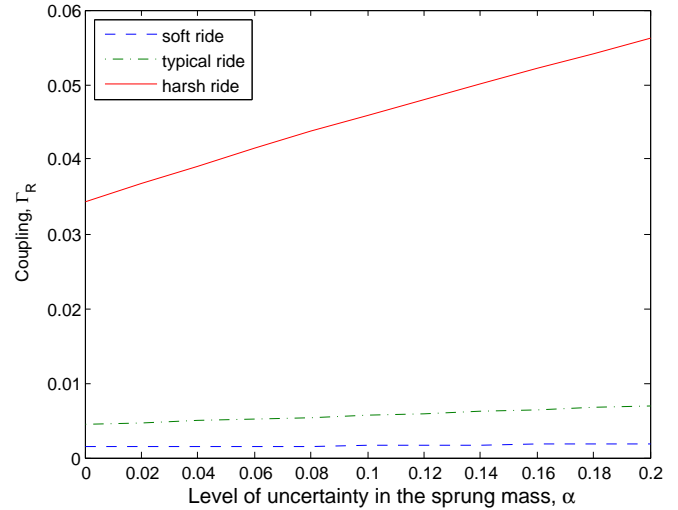


Fig. 2. Relationship between coupling and level of uncertainty for different ride characteristics

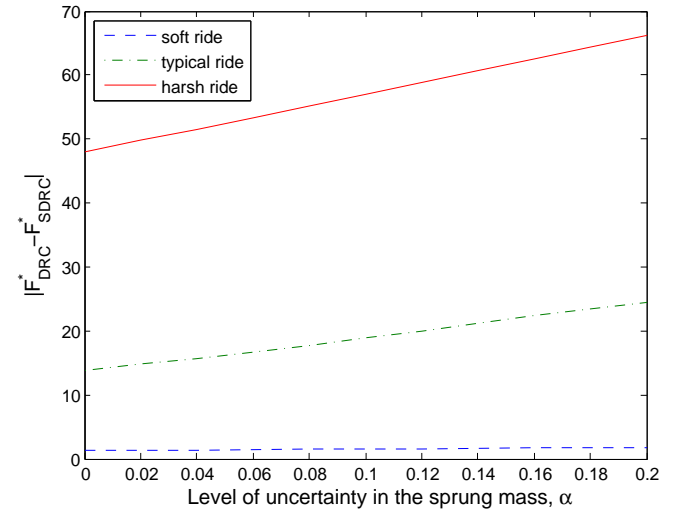


Fig. 3. Relationship between the absolute difference of DRC and SDRC optimal worst-case performances and level of uncertainty for different ride characteristics

a result, the increased demand for robustness for vehicle suspensions with harsh ride characteristics tend to increase coupling even further, so solving the DRC in Equation (4) is advantageous for high robustness requirements for the harsh ride case (DRC/H). On the other hand, the increased demand for robustness in vehicle suspensions with soft ride characteristics tends to increase coupling slightly with much lower slope than with typical and harsh ride characteristics. Hence, decoupled vehicle suspensions with soft ride characteristics tend to remain decoupled even with increased demand for robustness.

In summary, coupling between design and robust control tends to increase with the level of uncertainty applied. In addition, decoupled vehicle suspensions with soft ride characteristics tend to remain decoupled even with increased demand for robustness, while demanding more robustness for

vehicle suspensions with harsh ride characteristics increases coupling much more rapidly compared to suspensions with soft and typical ride characteristics.

B. Relationship Between Coupling and Robustness Resulting from Varying the Tire Stiffness and Unsprung Mass Parameters

The relationship between coupling and robustness can also be examined by varying a suspension system parameter. By fixing the level of uncertainty of the sprung mass α , the parameter value effect on coupling and robustness can be examined. Here, we investigate the effect of tire stiffness k_{us} and unsprung mass m_{us} on coupling and robustness. To that end, we assume that the level of uncertainty α is fixed at $\alpha = 0.2$ (i.e., 20% uncertainty). Moreover, let us consider the typical case (DRC/T) ride characteristic.

Following Alyaout [18], we first define our notion of control system robustness. Consider the following definition for worst-case control performance F_{DRC}^* obtained using the DRC strategy. Then control system robustness is defined as the reciprocal $1/F_{DRC}^*$. Note that decreasing F_{DRC}^* increases robustness. Hence, this definition is consistent because increasing $1/F_{DRC}^*$ increases robustness and vice-versa. Now we examine the relationship between the DRC coupling and the robustness of the control system.

Consider varying the tire stiffness k_{us} from 520 kN/m to 1600 kN/m. The relationship between coupling and robustness, obtained by varying the tire stiffness k_{us} , is illustrated in Figure 4. The DRC coupling has a monotonically increasing relationship with robustness, so decreasing coupling decreases robustness. Hence, there is a tradeoff between coupling and robustness. In this tradeoff, decreasing the tire stiffness k_{us} tends to decrease coupling at the cost of decreased robustness, while increasing k_{us} tends to increase robustness at the cost of increased coupling. Therefore, vehicle suspension systems with large tire stiffness tend to have improved robustness and large coupling, while suspension systems with small tire stiffness k_{us} tend to have small coupling and reduced robustness.

Now consider varying the unsprung mass m_{us} from 184 kg to 220 kg. Figure 5 shows the relationship between coupling and robustness obtained by varying the unsprung mass m_{us} . The DRC coupling has a monotonically decreasing relationship with robustness, so decreasing coupling increases robustness. Therefore, reducing the unsprung mass m_{us} improves both coupling and robustness while increasing the unsprung mass m_{us} increases coupling and reduces robustness. Therefore, vehicle suspension systems with small unsprung mass tend to have improved robustness and smaller coupling.

V. FREQUENCY RESPONSE

Now let us examine the robustness characteristics and the frequency response of the vehicle suspension problem with the typical case (DRC/T) ride characteristic ($r_0 = 1, r_1 = 1, r_2 = 2 \times 10^3, r_3 = 4 \times 10^{-8}$). A comparison between the passive solution, the nominal solution (i.e., zero

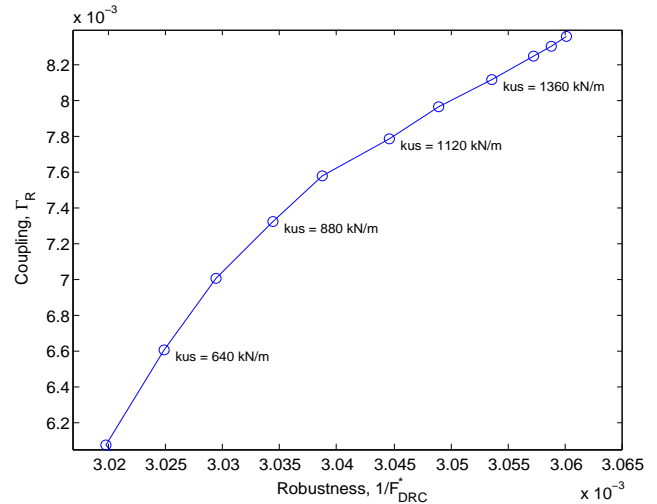


Fig. 4. Relationship between coupling and robustness resulting from varying the tire stiffness for the typical case (DRC/T) ride characteristic

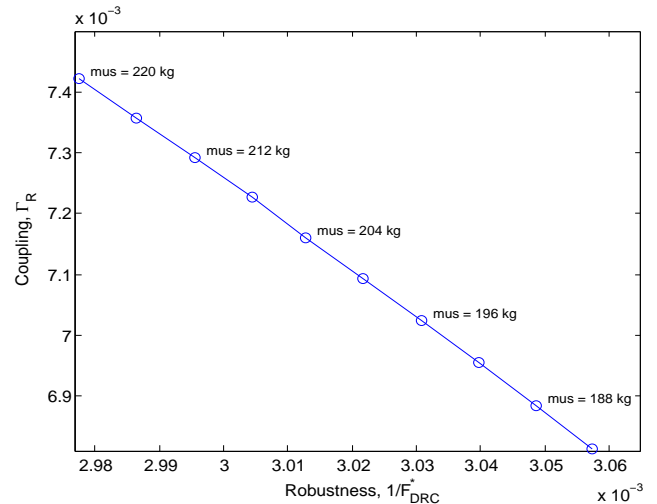


Fig. 5. Relationship between coupling and robustness resulting from varying the unsprung mass for the typical case (DRC/T) ride characteristic

TABLE II
PERFORMANCE AND ROBUSTNESS COMPARISON FOR THE TYPICAL RIDE CASE (DRC/ T)

Description	Passive	SDRC $\alpha = 0$	DRC $\alpha = 0$	SDRC $\alpha = 20$	DRC $\alpha = 20$
Susp. Performance, F	401.69	335.8	321.97	342.3	324.79
Susp. quality, J_q	401.69	324.22	315.81	323.7	318.32
Control energy, J_u (10^8)	0	2.894	1.5403	4.6353	1.6169
Worst Performance	446.2	360.69	334.58	353.89	329.43
Worst Susp. quality	446.2	349.88	329.7	336.22	324.47
Worst Control energy	0	2.703	1.222	4.4192	1.2403
k_s (kN/m)	1.204	1.204	18.55	1.204	16.86
c_s (kN.s/m)	7.953	7.953	3.045	7.953	2.17
Controller Gain, \mathbf{K}	0	55.4	63.15	45.69	63.17
	0	4.75	1.33	5.32	0.925
	0	81.8	64.78	66.95	63.83
	0	9.849	14.2	6.57	14.27
	0	-1.369	-2.12	-1.048	-1.76

uncertainty) obtained using the SDRC and DRC, and the robust solution (i.e., 20% uncertainty) obtained using the SDRC and DRC is shown in Table II. The nominal SDRC solution ($\alpha = 0$) yielded greatly improved performance and robustness over the passive design (no control energy applied), so going from passive design to active suspensions yielded the largest performance and robustness gains. The nominal DRC solution ($\alpha = 0$), to a lesser degree, improved performance and robustness compared the SDRC solution. The robust SDRC (i.e., 20% uncertainty) yielded improved robustness over the nominal SDRC (i.e., zero uncertainty) but worst robustness compared to the nominal DRC. The robust DRC yielded the best robustness at the expense of incurring a small loss compared to the nominal DRC.

The suspension quality spectral density is an aggregate frequency-domain measure of the strengths of the signals contributing to suspension quality, assuming unity disturbance variance ($2\pi A_0 V = 1$). The suspension quality is defined as $J_q = E(\int_{t_i}^{t_f} (r_0 \ddot{x}_s^2 + r_1 (x_{us} - x_0)^2 + r_2 (x_s - x_{us})^2) dt)$. Figure 6 compares the suspension quality spectral density for the passive and actively controlled suspensions obtained using the SDRC and DRC strategies. At low frequencies, the nominal DRC achieves lower suspension quality than the robust DRC. In addition, all nominal and robust SDRC and DRC strategies achieve low suspension quality at low frequencies compared to the passive at the expense of higher suspension quality in the frequency range 3-10 (rad/s).

The control energy spectral density is a frequency-domain measure of the control energy ($J_u = E(\int_{t_i}^{t_f} u^2 dt)$), assuming unity disturbance variance. Figure 7 shows the control energy spectral density for the passive and actively controlled suspensions. At low frequencies, the nominal and robust DRC's seem to consume much more energy than the nominal and robust SDRC's, so much of the nominal and robust DRC's low energy consumption is concentrated in the frequency range 1-100 (rad/s). In addition, the robust DRC

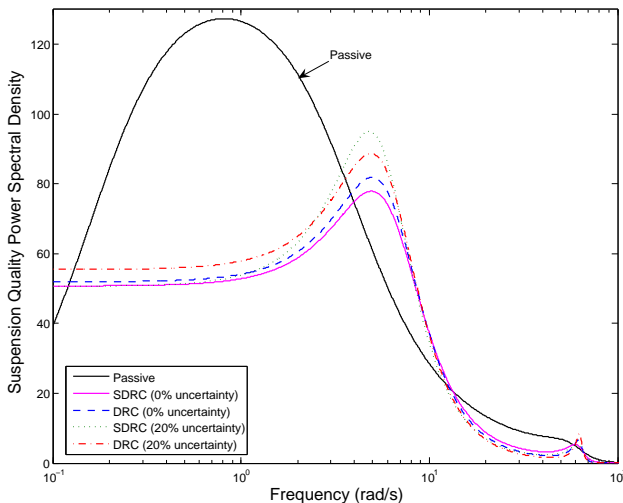


Fig. 6. Suspension quality spectral density

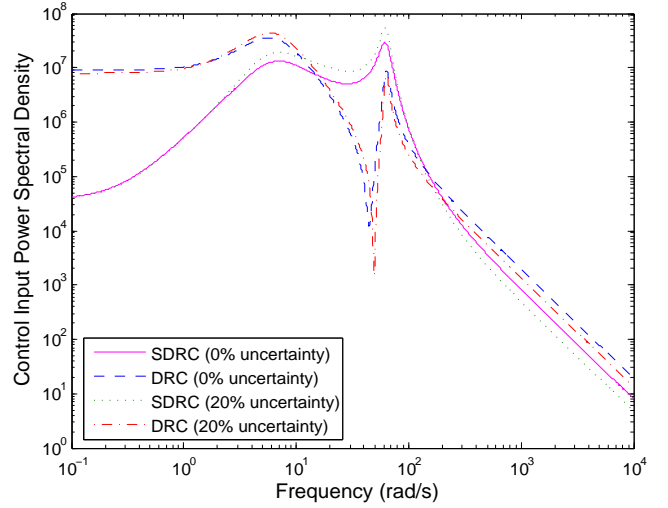


Fig. 7. Control input spectral density

and nominal DRC have almost identical frequency response; similarly, the robust SDRC and nominal SDRC have identical response at low frequencies.

VI. CONCLUSION

This article introduced a worst-case approach that combined passive and active elements to improve the robustness of a vehicle suspension system. This is achieved by examining the relationship between coupling and robustness resulting from varying different suspension parameters. This link between coupling and robustness is utilized in assessing the parameters' influence on coupling and robustness.

By varying the level of uncertainty parameter, we showed that the coupling between design and robust control tended to increase as the applied level of uncertainty increased. Therefore, designers of active/passive suspensions who demand more robustness should consider solving the DRC because the SDRC will not necessarily improve robustness due to the coupling increase. In addition, demanding more robustness for vehicle suspensions with harsh ride characteristics increased coupling much more rapidly compared to suspensions with soft ride characteristics.

We then examined the effect of tire stiffness k_{us} and unsprung mass m_{us} on coupling and robustness. For the tire stiffness, vehicle suspension systems with large tire stiffness tend to have improved robustness but large coupling, while suspension systems with small tire stiffness k_{us} tend to have small coupling but reduced robustness. As for the unsprung mass, vehicle suspension systems with small unsprung mass m_{us} tend to have both improved robustness and smaller coupling.

Future work should consider including uncertainties in variables and parameters other than the sprung mass m_s . Future work should also consider optimizing coupling to improve robustness as opposed to solving the DRC optimization problem.

REFERENCES

- [1] D. Hrovat, "Applications of optimal control to advanced automotive suspension design," *Journal of Dynamic Systems, Measurement and Control*, vol. 115, pp. 328–342, 1993.
- [2] —, "Survey of advanced suspension developments and related optimal control applications," *Automatica*, vol. 33, pp. 1781–1817, 1997.
- [3] H. K. Fathy, P. Y. Papalambros, A. G. Ulsoy, and D. Hrovat, "Nested plant/controller optimization with application to combined passive/active automotive suspensions," *American Control Conference*, Denver, CO, June 4-6, vol. 4, pp. 3375–3380, 2003.
- [4] M. C. Smith and G. W. Walker, "Performance limitations and constraints for active and passive suspensions: A mechanical multi-port approach," *Vehicle System Dynamics*, vol. 33, pp. 137–168, 2000.
- [5] A. G. Ulsoy, D. Hrovat, and T. Tseng, "Stability robustness of LQ and LQG active suspensions," *Journal of Dynamic Systems, Measurement and Control*, vol. 116, pp. 123–131, 1994.
- [6] A. G. Ulsoy and D. Hrovat, "Stability robustness of LQG active suspensions," *American Control Conference*, San Diego, CA, May 23-25, vol. 2, pp. 1347–1356, 1990.
- [7] S. Chantranuwathana and H. Peng, "Adaptive robust force control for vehicle active suspensions," *International Journal of Adaptive Control and Signal Processing*, vol. 18, pp. 83–102, 2004.
- [8] I. Fialho and G. Balas, "Design of nonlinear controllers for active vehicle suspensions using parameter-varying control synthesis," *Vehicle System Dynamics*, vol. 33, pp. 351–370, 2000.
- [9] C. Lauwerys, J. Swevers, and P. Sas, "Robust linear control of an active suspension on a quarter car test-rig," *Control Engineering Practice*, vol. 13, pp. 577–586, 2005.
- [10] L. Ray, "Robust linear-optimal control laws for active suspension systems," *Journal of Dynamic Systems, Measurement and Control*, vol. 114, pp. 592–598, 1992.
- [11] H. Chen and G. Kong-Hui, "Constrained \mathcal{H}_∞ control of active suspensions: An LMI approach," *IEEE Transactions on Automatic Control*, vol. 13, pp. 412–421, 2005.
- [12] K. Hayakawa, K. Matsumoto, M. Yamashita, Y. Suzuki, K. Fujimori, and K. Hayakawa, "Robust \mathcal{H}_∞ output feedback control of decoupled automobile active suspension systems," *IEEE Transactions on Automatic Control*, vol. 44, pp. 392–396, 1999.
- [13] I. Petersen, V. Ugrinovski, and A. Savkin, *Robust Control Design Using \mathcal{H}_∞ Methods*. London, UK: Springer-Verlag, 2000.
- [14] J. Onoda and R. T. Haftka, "Approach to structure/control simultaneous optimization for large flexible spacecraft," *AIAA Journal*, vol. 25, pp. 1133–1138, 1987.
- [15] G. P. O'Neal, B.-K. Min, Z. J. Pasek, and Y. Koren, "Integrated structural/control design of micro-positioner for boring bar tool insert," *Journal of Intelligent Material Systems and Structures*, vol. 12, pp. 617–627, 2001.
- [16] S. Alyaqout, P. Y. Papalambros, and A. G. Ulsoy, "Combined robust design and robust control of an electric DC motor," *ASME International Mechanical Engineering Congress and Exposition*, Chicago, Illinois, November 5-10, vol. IMECE2006-16027, 2006.
- [17] —, "Quantification and use of system coupling in decomposed design optimization problems," *ASME International Mechanical Engineering Congress and Exposition*, Orlando, Florida, November 5-11, vol. IMECE2005-81364, 2005.
- [18] S. Alyaqout, "A multi-system optimization approach to coupling in robust design and control," Doctoral dissertation, Dept. of Mechanical Engineering, University of Michigan, Ann Arbor, 2006.
- [19] J. A. Reyer, H. K. Fathy, P. Y. Papalambros, and A. G. Ulsoy, "Comparison of combined embodiment design and control optimization strategies using optimality conditions," *ASME Design Engineering Technical Conferences*, Pittsburgh, PA, September 9-12, vol. 2, pp. 1023–1032, 2001.
- [20] H. K. Fathy, J. A. Reyer, P. Y. Papalambros, and A. G. Ulsoy, "On the coupling between the plant and controller optimization problems," *American Control Conference*, Arlington, VA, June 25-27, vol. 3, pp. 1864–1869, 2001.